

ILC Cosmology *

Jonathan L. Feng

Department of Physics and Astronomy, University of California, Irvine, CA 92697, USA

Recent breakthroughs in cosmology pose questions that require particle physics answers. I review the problems of dark matter, baryogenesis, and dark energy and discuss how particle colliders, particularly the International Linear Collider, may advance our understanding of the contents and evolution of the Universe.

1. INTRODUCTION

We are living through a period of scientific revolution: for the first time in history, we have a compelling picture of the Universe on the largest scales. At the same time, we are preparing for a revolution in particle physics as we explore the weak scale at the Tevatron, the Large Hadron Collider (LHC), and the proposed International Linear Collider (ILC). Here I present one view of how these two revolutions might be related.

In recent years, observations of supernovae, the cosmic microwave background (CMB), and galaxy clusters have provided three stringent constraints on Ω_M and Ω_Λ , the energy densities of matter and dark energy in units of the critical density. These results are consistent and favor $(\Omega_M, \Omega_\Lambda) \approx (0.3, 0.7)$, as shown in Fig. 1. The amount of matter in the form of baryons is also constrained, both by the CMB and by the observed abundances of light elements together with the theory of Big Bang nucleosynthesis (BBN). Although there are at present possibly significant disagreements within the BBN data, the CMB and BBN data taken as a whole are also impressively consistent, providing yet another success for the current standard model of cosmology.

Through these and many other observations, the total energy densities of non-baryonic dark matter, baryons, and dark energy are constrained to be [2, 3]

$$\Omega_{DM} = 23\% \pm 4\% \quad (1)$$

$$\Omega_B = 4\% \pm 0.4\% \quad (2)$$

$$\Omega_\Lambda = 73\% \pm 4\% . \quad (3)$$

These results are remarkable. In particular, Ω_Λ is larger than many expected, with profound implications for what the cosmological constant problem is and how it might be solved. At least two of the constraints of Fig. 1 must be wrong to change this conclusion. These results are also remarkably precise — the fractional uncertainties on all three are $\mathcal{O}(10\%)$. Given that just a decade ago the range $0.2 \lesssim \Omega_{DM} \lesssim 0.6$ was allowed and $\Omega_\Lambda = 0$ was often assumed, this represents spectacular progress. Although much of cosmology remains imprecise, as we will see, the quantum leap in precision in these three quantities already has dramatic implications for particle physics.

At the same time, recent progress in cosmology is probably best viewed as the first steps on the road to understanding the Universe. Consider an historical precedent: in 200 B.C., Eratosthenes determined the size of the Earth. On a day when the Sun was directly overhead in Syene, Eratosthenes sent a graduate student to measure the lengths of shadows in Alexandria. He was then able to extrapolate from the known distance between these two cities to determine the circumference of the Earth. His answer was

$$2\pi R_\oplus = 250,000 \text{ stadia} . \quad (4)$$

*Plenary Colloquium presented at the 2005 International Linear Collider Workshop, Stanford, California, USA, 18-22 March 2005.

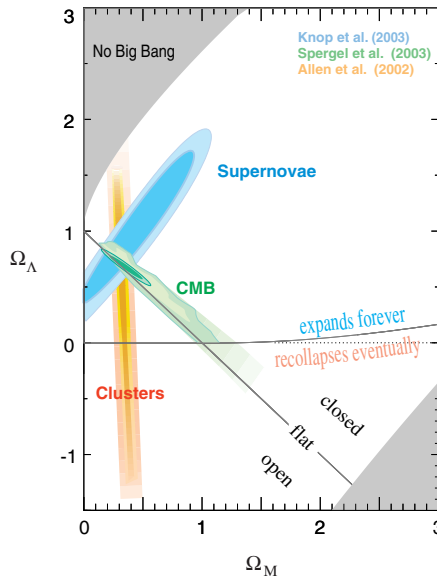


Figure 1: Constraints on Ω_M and Ω_Λ from observations of supernovae, the CMB, and galaxy clusters [1].

This result is remarkable. At the time of publication, it was bigger than many expected, leading many to be skeptical and helping to earn Eratosthenes the nickname “Beta” [4]. His result was also remarkably precise. We now know that it was good to less than 10% [5, 6, 7], where the leading source of uncertainty is systematic error from the exact definition of the unit “stadion” [8]. At the same time, the achievement of Eratosthenes, though important, could hardly be characterized as a complete understanding of the Earth. Rather, it was just the beginning of centuries of exploration, which eventually led to the mapping of continents and oceans, giving us the picture of the Earth we have today.

In a similar vein, recent breakthroughs in cosmology answer many questions, but highlight even more. These include

- Dark Matter: What is it? How is it distributed? How does it impact structure formation?
- Baryons: Why is there an asymmetry between matter and anti-matter? Why does Ω_B have the value it has?
- Dark Energy: What is it? Why isn’t $\Omega_\Lambda \sim 10^{120}$? Why isn’t Ω_Λ zero? How does it evolve?

Although these questions will continue to be sharpened by astrophysical observations at large length scales, it is clear that satisfying answers will require fundamental progress in our understanding of microphysics. This is nothing new — the history of advances in cosmology is to a large extent the story of successful synergy between studies of the Universe on the smallest and largest length scales. This interplay is shown in Fig. 2, where several milestones in particle physics and cosmology are placed along the cosmological timeline. As particle experiments reach smaller length scales and higher energies, they probe times closer to the Big Bang. Just as atomic physics is required to interpret the CMB signal from $t \sim 10^{13}$ s after the Big Bang and nuclear physics is required to extrapolate back to BBN at $t \sim 1$ s, particle physics, and particularly the physics of the electroweak scale, is required to understand the era before $t \sim 10^{-8}$ s, the era that contains the answers to many of our most basic questions.

In the next few years, the Tevatron and LHC will play the crucial role of opening the door to the weak scale, to be followed, we hope, by detailed studies of new physics at these colliders and the proposed ILC. Here I will give an overview of the potential role of particle colliders, and especially the ILC, in answering cosmological questions. The discussion begins with dark matter, a subject in which there are many concrete and compelling connections between the ILC and cosmology. We will then consider baryogenesis and dark energy. Much of the work described here is an outgrowth of the activities of the Cosmology Subgroup of the American Linear Collider Physics Group. Additional

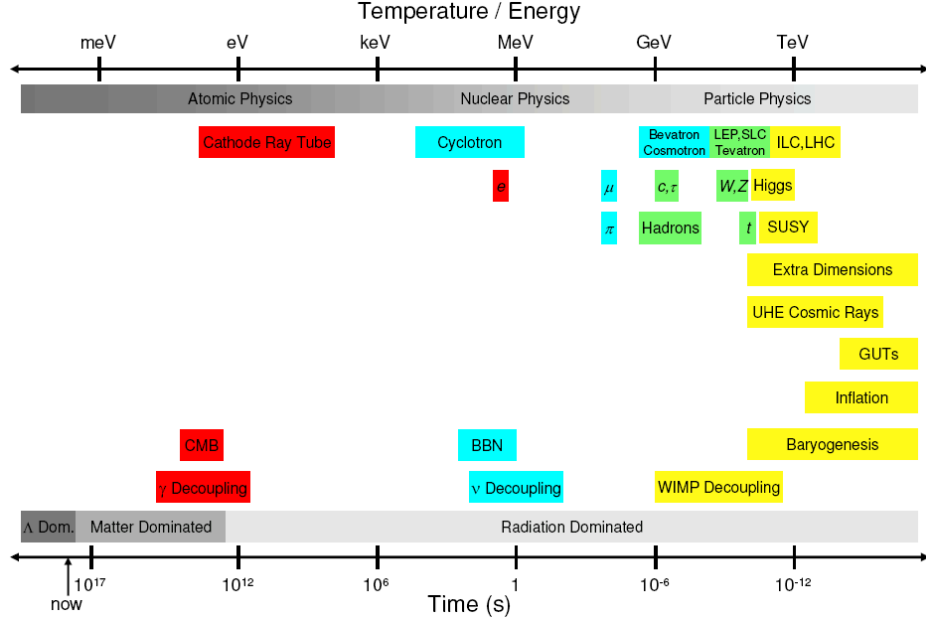


Figure 2: Milestones in particle physics and cosmology along the cosmological timeline.

background and results may be found in the Cosmology Subgroup’s report [9], as well as in other contributions to the proceedings of this workshop [10, 11, 12, 13, 14, 15, 16].

2. DARK MATTER

2.1. Dark Matter and the Weak Scale

The particle or particles that make up most of dark matter must be stable, at least on cosmological time scales, and non-baryonic, so that they do not disrupt the successes of BBN. They must also be cold or warm to properly seed structure formation, and their interactions with normal matter must be weak enough to avoid violating current bounds from dark matter searches. The stringency of these criteria pale in comparison with the unbridled enthusiasm of theorists, who have proposed scores of viable candidates with masses and interaction cross sections varying over tens of orders of magnitude.

Candidates with weak scale masses have received much of the attention, however. There are at least four good reasons for this. First, these proposals are testable. Second, new particles at the weak scale are independently motivated by attempts to understand electroweak symmetry breaking. Third, these new particles often “automatically” have all the right properties to be dark matter. For example, their stability often follows as a result of discrete symmetries that are necessary to make electroweak theories viable, independent of cosmology. And fourth, these new particles are naturally produced with the cosmological densities required of dark matter.

The last motivation is particularly tantalizing. Dark matter may be produced in a simple and predictive manner as a thermal relic of the Big Bang. The evolution of a thermal relic’s number density is shown in Fig. 3. In stage (1), the early Universe is dense and hot, and all particles are in thermal (chemical) equilibrium. In stage (2), the Universe cools to temperatures T below the dark matter particle’s mass m_χ , and the number of dark matter particles becomes Boltzmann suppressed, dropping exponentially as $e^{-m_\chi/T}$. In stage (3), the Universe becomes so cool and dilute that the dark matter annihilation rate is too low to maintain equilibrium. The dark matter particles then “freeze out,” with their number asymptotically approaching a constant, their thermal relic density.

More detailed analysis shows that the thermal relic density is rather insensitive to m_χ and inversely proportional

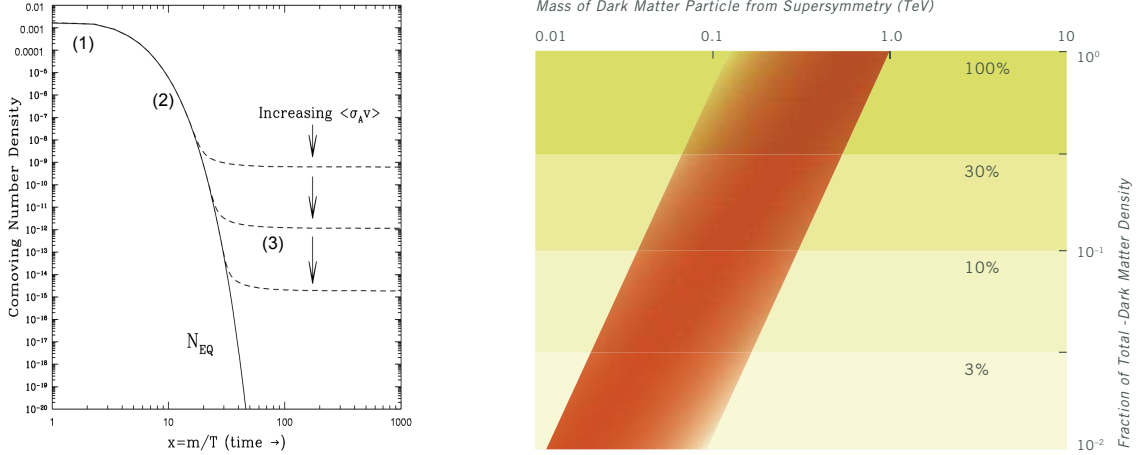


Figure 3: Left: The cosmological evolution of a thermal relic’s comoving number density [17]. Right: A band of natural values in the (m_χ, Ω_χ) plane for a thermal relic [18].

to the annihilation cross section: $\Omega_{\text{DM}} \sim \langle \sigma_A v \rangle^{-1}$. The constant of proportionality depends on the details of the microphysics, but we may give a rough estimate. On dimensional grounds, the cross section can be written

$$\sigma_A v = k \frac{4\pi\alpha_1^2}{m_\chi^2} (1 \text{ or } v^2) , \quad (5)$$

where v is the relative velocity of the annihilating particles, the factor v^2 is absent or present for S - or P -wave annihilation, respectively, and terms higher-order in v have been neglected. The constant α_1 is the hypercharge fine structure constant, and k parameterizes deviations from this estimate.

With this parametrization, given a choice of k , the relic density is determined as a function of m_χ . The results are shown in Fig. 3. The width of the band comes from considering both S - and P -wave annihilation, and from letting k vary from $\frac{1}{2}$ to 2. We see that a particle that makes up all of dark matter is predicted to have mass in the range $m_\chi \sim 100 \text{ GeV} - 1 \text{ TeV}$; a particle that makes up 10% of dark matter, still significant with respect to its impact on structure formation, for example, has mass $m_\chi \sim 30 \text{ GeV} - 300 \text{ GeV}$. There are models in which the effective k is outside our illustrative range. In fact, values of k smaller than we have assumed, predicting smaller m_χ , are not uncommon, as the masses of virtual particles in annihilation diagrams can be significantly higher than m_χ . However, the general conclusion remains: particles with mass at the weak scale naturally have significant thermal relic densities. For this reason, even null results from LHC and ILC searches for dark matter are important, and a thorough exploration of the weak scale will play a crucial role in attempts to identify the particle or particles that make up dark matter.

Given these results, many theories for new physics at the weak scale contain promising dark matter candidates. The candidates that exploit the tantalizing numerical “coincidence” shown in Fig. 3 may be grouped into two classes: WIMPs and superWIMPs [19]. In the following subsections, we consider what insights colliders may provide in each of these two cases.

2.2. WIMPs

Weakly-interacting massive particles (WIMPs) have weak-scale masses and weak-scale interactions. They include neutralinos in supersymmetry [20], Kaluza-Klein particles in theories with universal extra dimensions [21, 22], branons in theories with large extra dimensions [23], and the lightest T -odd particle in some little Higgs theories [24].

The study of WIMP dark matter at colliders may be divided into three (overlapping) stages:

1. WIMP Candidate Identification. Is there evidence for WIMPs from colliders from, for example, events with missing energy and momentum? What are the candidates’ masses, spins, and other quantum numbers?

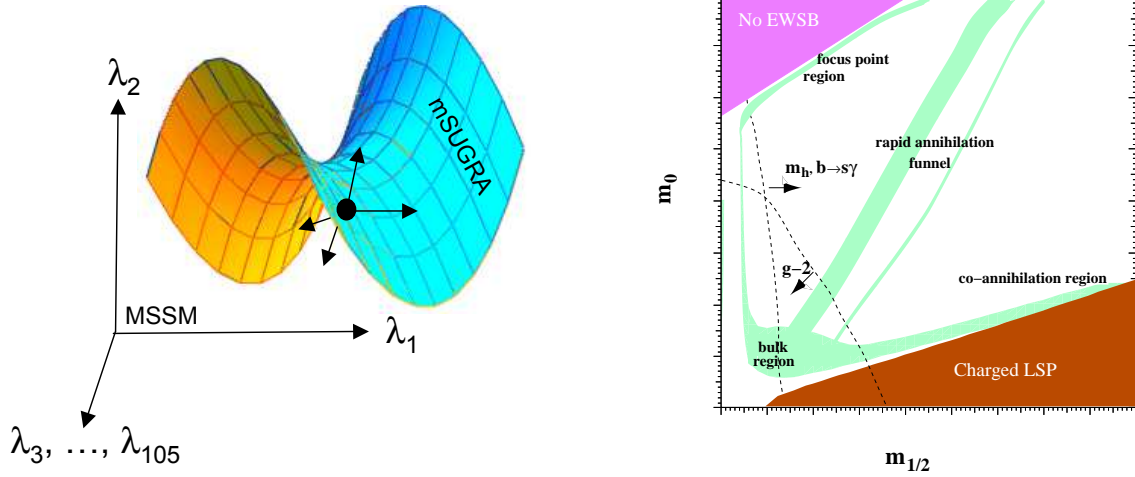


Figure 4: Left: Minimal supergravity (mSUGRA) defines a hypersurface in the 105-dimensional parameter space of the MSSM. In the studies described here, the underlying parameters are assumed to lie on the mSUGRA hypersurface, but deviations in all directions of the MSSM parameter space are allowed when evaluating the potential of colliders to constrain parameters. Right: Schematic diagram of regions with the right amount of dark matter (shaded) in mSUGRA. This diagram is qualitative. The locations of the shaded regions depend on suppressed parameters, and axis labels are purposely omitted [9].

2. WIMP Relic Density Determination. What are the dark matter candidates' predicted thermal relic densities? Can they be significant components or all of dark matter?
3. Mapping the WIMP Universe. Combined with results from direct and indirect dark matter searches, what can collider studies tell us about astrophysical questions, such as the distribution of dark matter in the Universe?

Stage 1 is discussed in Ref. [9]. In the following subsections, we will explore how well the LHC and ILC may advance Stages 2 and 3.

To address these issues concretely, it is necessary to focus on one representative example, typically neutralinos. Even with this restriction, there are many qualitatively different scenarios. A common choice is to study minimal supergravity (mSUGRA), a simple model framework that encompasses many different possibilities. In this case, one assumes that the underlying supersymmetry parameters realized in Nature are those of a point in mSUGRA parameter space. In determining the capabilities of colliders, however, it is best to relax all mSUGRA assumptions and ask how well the 105 parameters of the general Minimal Supersymmetric Standard Model (MSSM) may be determined. This approach is illustrated in Fig. 4.

In much of mSUGRA parameter space the neutralino relic density lies above the narrow allowed window, and so these possibilities are cosmologically excluded. The regions in which the neutralino relic density is not too large, but is still sufficient to be all of dark matter, are cosmologically preferred. They have been given names and include the bulk, focus point, co-annihilation, and rapid annihilation funnel regions shown in Fig. 4. Results from representative models in each of the first two regions are summarized below. For results for the other two regions and related studies, see Refs. [10, 13, 16, 25, 26]. For each model, the superpartner spectrum is determined by ISAJET [27], and cosmological observables, such as the thermal relic density, are determined by DARKSUSY [28] and micrOMEGAs [29].

2.2.1. WIMP Relic Density Determination

A. Bulk Region

In the bulk region, a much studied model is specified by the mSUGRA parameters

$$\text{LCC1: } (m_0, M_{1/2}, A_0, \tan\beta) = (100 \text{ GeV}, 250 \text{ GeV}, -100 \text{ GeV}, 10) \quad [\mu > 0, m_{3/2} > m_{\text{LSP}}, m_t = 178 \text{ GeV}] . \quad (6)$$

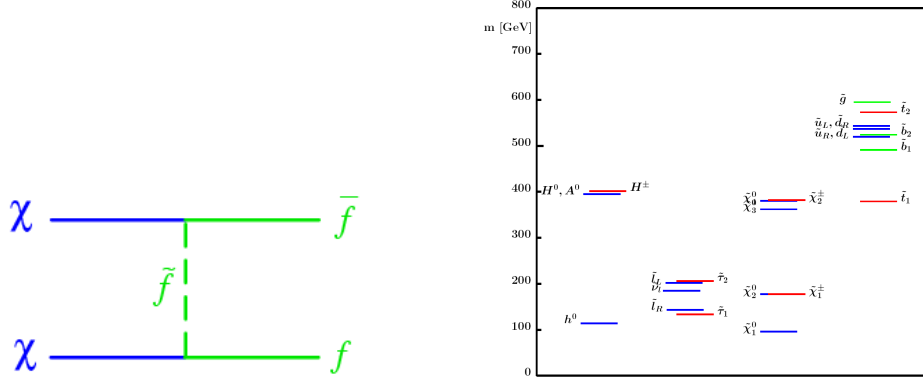


Figure 5: Left: The dominant neutralino annihilation process in the bulk region. Right: The superpartner spectrum at LCC1, a representative model in the bulk region [30].

The neutralino thermal relic density at this point is $\Omega_\chi h^2 = 0.19$ ($h \simeq 0.71$), significantly higher than allowed by the latest cosmological constraints. Nevertheless, the choice of LCC1 is convenient, since it has been studied in great detail in other studies, where it is also known as SPS1a [30].

In the bulk region, neutralinos annihilate dominantly through $\chi\chi \rightarrow f\bar{f}$ through a t -channel scalar \tilde{f} , as shown in Fig. 5. To achieve the correct relic density, this process must be efficient, requiring light sfermions and, since the neutralino must be the lightest supersymmetric particle (LSP), light neutralinos. These characteristics are exhibited in the superpartner spectrum of LCC1, shown in Fig. 5. It is noteworthy that in this case, cosmology provides a strong motivation for light superpartners within the reach of a 500 GeV ILC.

To determine the relic density at LCC1, all of the supersymmetry parameters entering annihilation processes, including those shown in Fig. 5 and others, must be determined to high accuracy. The LCC1 superpartner spectrum makes possible many high precision measurements at the LHC. LCC1 (SPS1a) is in significant respects a “best case scenario” for the LHC. The implications of these measurements for cosmology will be summarized below.

The LHC results may be improved at the ILC. For example, superpartner masses may be determined with extraordinary precision through kinematic endpoints and threshold scans, as shown in Fig. 6. The kinematic endpoints of final state leptons in the process $e^+e^- \rightarrow \tilde{l}^+\tilde{l}^- \rightarrow l^+l^-\chi\chi$ determine both \tilde{l} and χ masses. Slepton masses may also be determined through threshold scans. Threshold scans provide even higher precision, and may actually *save* luminosity. This is the case, for example, for selectron mass determinations through e^-e^- threshold scans, where precisions of tens of MeV may be obtained with 1 to 10 fb $^{-1}$ of integrated luminosity [32, 33, 34]. More generally, the required measurements exploit the full arsenal of the ILC, from its variable beam energy, to its polarized beams, to the e^-e^- option. The results of one study are summarized in Fig. 7.

The neutralino thermal relic density may be determined by combining the precise determination of all relevant supersymmetry parameters and also verifying the insensitivity of the relic density to all other parameters. The results depend somewhat on the prescription one uses to combine these data. One approach is to choose points in parameter space at random, weighting each with a Gaussian distribution for each observable. The relic density allowed region is then identified as the symmetric interval around the central value that contains 68% of the weighted probability.

The result of applying this method with 50,000 scan points around LCC1 is shown in Fig. 8. The result is that the ILC may determine the thermal relic density to a fractional uncertainty of

$$\text{LCC1 (preliminary): } \frac{\Delta(\Omega_\chi h^2)}{\Omega_\chi h^2} = 2.2\% \quad [\Delta(\Omega_\chi h^2) = 0.0042]. \quad (7)$$

The current constraint from WMAP, as well as projected future constraints on cosmological observations from the Planck satellite (both scaled up to the LCC1 central value for Ω_χ) are also shown. WMAP and Planck provide no information about the mass of the dark matter particle.

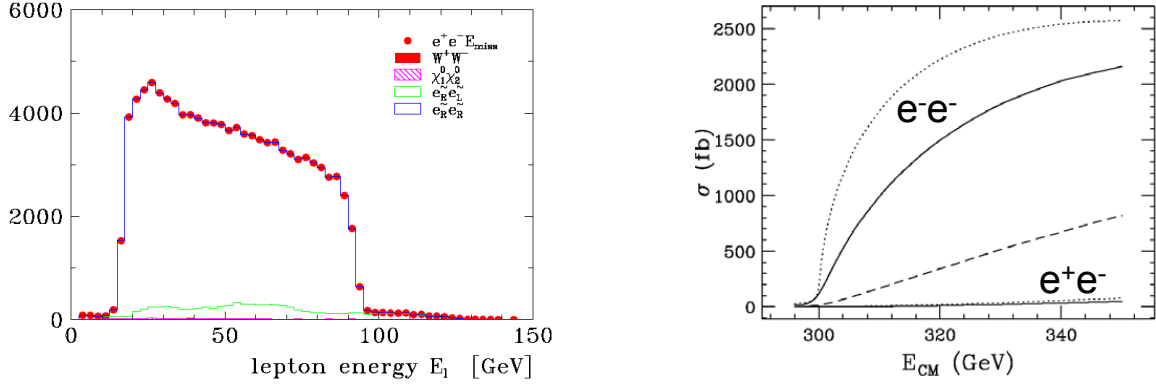


Figure 6: Left: The kinematic endpoints of lepton energies from $e^+e^- \rightarrow \tilde{l}^+\tilde{l}^- \rightarrow l^+l^-\chi\chi$ provide precise determinations of slepton and neutralino masses [31]. Right: Threshold scans may also be used to determine slepton masses. In the case of selectron masses, e^-e^- threshold scans provide higher precision and simultaneously *save* luminosity [33].

	m [GeV]	Δm [GeV]	Comments
$\tilde{\chi}_1^\pm$	176.4	0.55	simulation threshold scan, 100 fb $^{-1}$
$\tilde{\chi}_2^\pm$	378.2	3	estimate $\tilde{\chi}_1^\pm\tilde{\chi}_2^\mp$, spectra $\tilde{\chi}_2^\pm \rightarrow Z\tilde{\chi}_1^\pm, W\tilde{\chi}_1^0$
$\tilde{\chi}_1^0$	96.1	0.05	combination of all methods
$\tilde{\chi}_2^0$	176.8	1.2	simulation threshold scan $\tilde{\chi}_2^0\tilde{\chi}_2^0$, 100 fb $^{-1}$
$\tilde{\chi}_3^0$	358.8	3–5	spectra $\tilde{\chi}_3^0 \rightarrow Z\tilde{\chi}_{1,2}^0, \tilde{\chi}_2^0\tilde{\chi}_3^0, \tilde{\chi}_3^0\tilde{\chi}_4^0$, 750 GeV, > 1000 fb $^{-1}$
$\tilde{\chi}_4^0$	377.8	3–5	spectra $\tilde{\chi}_4^0 \rightarrow W\tilde{\chi}_1^\pm, \tilde{\chi}_2^0\tilde{\chi}_4^0, \tilde{\chi}_3^0\tilde{\chi}_4^0$, 750 GeV, > 1000 fb $^{-1}$
\tilde{e}_R	143.0	0.05	e^-e^- threshold scan, 10 fb $^{-1}$
\tilde{e}_L	202.1	0.2	e^-e^- threshold scan 20 fb $^{-1}$
$\tilde{\nu}_e$	186.0	1.2	simulation energy spectrum, 500 GeV, 500 fb $^{-1}$
$\tilde{\mu}_R$	143.0	0.2	simulation energy spectrum, 400 GeV, 200 fb $^{-1}$
$\tilde{\mu}_L$	202.1	0.5	estimate threshold scan, 100 fb $^{-1}$ [36]
$\tilde{\tau}_1$	133.2	0.3	simulation energy spectra, 400 GeV, 200 fb $^{-1}$
$\tilde{\tau}_2$	206.1	1.1	estimate threshold scan, 60 fb $^{-1}$ [36]
\tilde{t}_1	379.1	2	estimate b -jet spectrum, $m_{\min}()$, 1TeV, 1000 fb $^{-1}$

Figure 7: The precision with which supersymmetry parameters may be determined at the ILC [31].

B. Focus Point Region

In the focus point region, one may choose the representative model

$$\text{LCC2: } (m_0, M_{1/2}, A_0, \tan\beta) = (3280 \text{ GeV}, 300 \text{ GeV}, 0, 10) \quad [\mu > 0, m_{3/2} > m_{\text{LSP}}, m_t = 175 \text{ GeV}] . \quad (8)$$

In focus point supersymmetry [35, 36], squarks and sleptons are very heavy, and so the diagrams that are dominant in the bulk region are suppressed.¹ Nevertheless, the desired relic density may be achieved [38], because in the focus point region, the neutralino is not a pure Bino, but contains a significant Higgsino component. The processes $\chi\chi \rightarrow W^+W^-$, shown in Fig. 9, and $\chi\chi \rightarrow ZZ$, which are negligible in the bulk region, therefore become efficient. Neutralino mixing is typically achieved when neutralinos and charginos are fairly light and not too split in mass, and so the demands of neutralino dark matter motivate supersymmetry with light neutralinos and charginos.

Determination of the thermal relic density in the focus point region requires precise measurements of neutralino and chargino masses and their mixings. Applying the method described above for converting collider constraints to a constraint on the thermal relic density, the thermal relic density may be determined with fractional uncertainty

$$\text{LCC2 (preliminary): } \frac{\Delta(\Omega_\chi h^2)}{\Omega_\chi h^2} = 2.4\% \quad [\Delta(\Omega_\chi h^2) = 0.0026] . \quad (9)$$

¹As a result of this property, models like focus point supersymmetry may be challenging for supersymmetry discovery and study at the LHC [37].

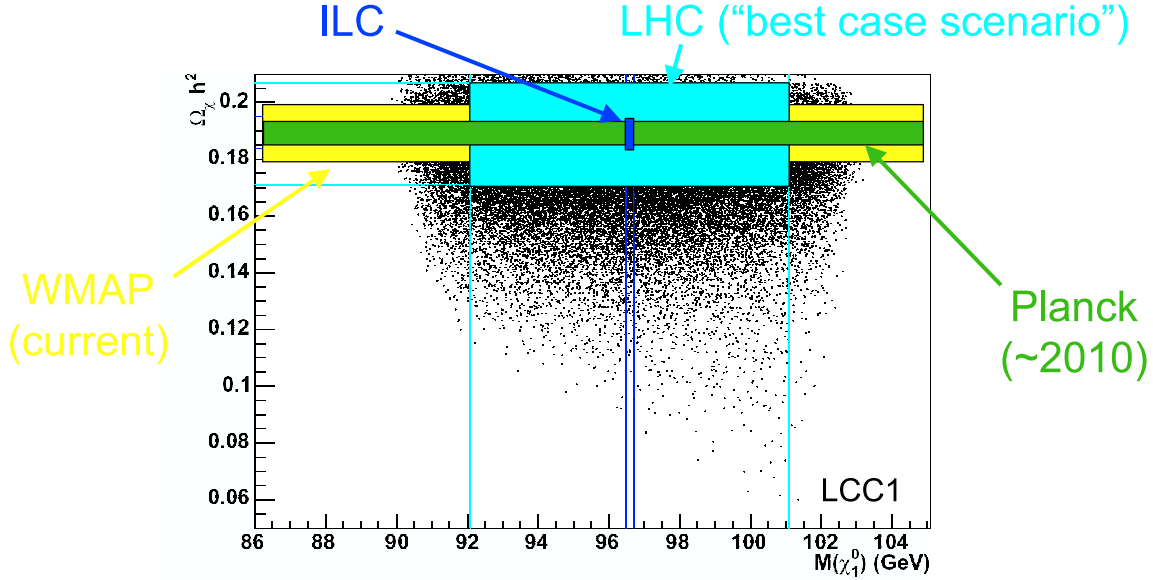


Figure 8: Constraints in the (m_χ, Ω_χ) plane from the ILC and LHC, with constraints on Ω_χ from the WMAP and Planck satellite experiments. The 50,000 scan points used to determine the ILC constraint are also shown (see text) [9]. Note that the distribution of scan points is much broader than the final ILC constrained region; out-lying points have very little probability weight.

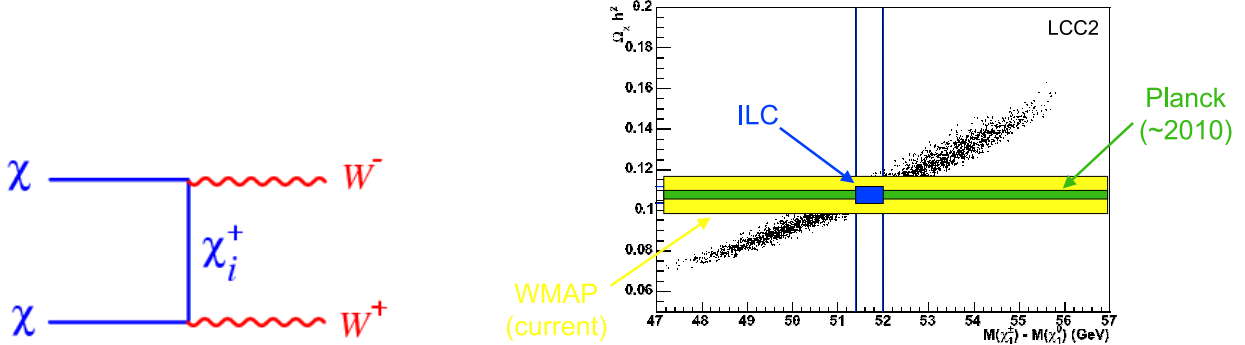


Figure 9: Left: The dominant neutralino annihilation process in the focus point region. Right: Constraints on the relic density from the ILC, WMAP, and Planck, as in Fig. 8 [9].

C. What We Learn

The results of Figs. 8 and 9 imply that the ILC will provide a part per mille determination of $\Omega_\chi h^2$ in these cases, matching WMAP and even the extraordinary precision expected from Planck. The many possible implications of such measurements are outlined in the flowchart of Fig. 10.

Consistency of the ILC and WMAP/Planck measurements at the part per mille level would provide strong evidence that neutralinos are absolutely stable and form all of the non-baryonic dark matter. Such a result would at last provide convincing evidence that we have produced dark matter at colliders and that we have identified its microphysical properties. It would be a landmark success of the particle physics/cosmology connection, and would give us confidence in our understanding of the Universe back to neutralino freeze out at $t \sim 10^{-8}$ s, eight orders of magnitude earlier than can currently be claimed.

On the other hand, inconsistency would lead to a Pandora's box of possibilities, all with important implications. If the thermal relic density determined from high energy physics is smaller than what is required cosmologically, these high precision measurements imply that neutralinos are at most only one component of cold, non-baryonic

IDENTIFYING DARK MATTER

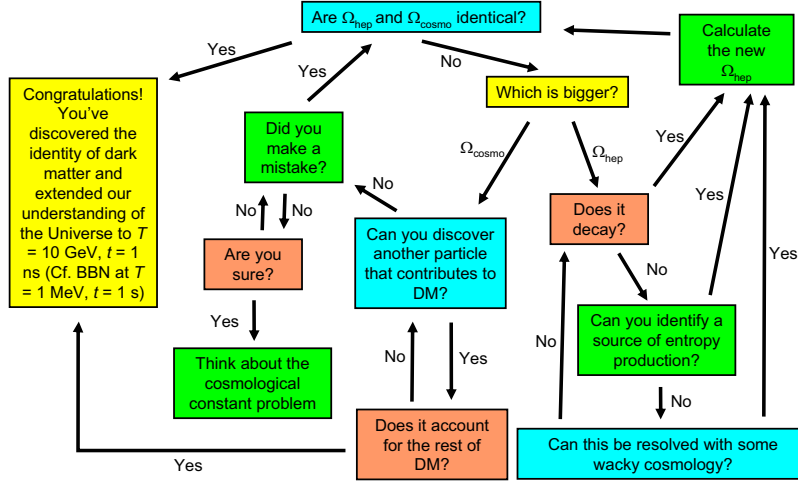


Figure 10: Flowchart illustrating the possible implications of comparing Ω_{hep} , the predicted dark matter thermal relic density determined from high energy physics, and Ω_{cosmo} , the actual dark matter relic density determined by cosmological observations.

dark matter. On the other hand, if the thermal relic density determined at colliders is too large, these measurements imply that neutralinos must decay (perhaps to superWIMPs — see below), or that the neutralino thermal relic density is diluted by entropy production or some other effect after freeze out.

The implications of LHC precision measurements for the relic density, determined in the way discussed above, are also shown in Fig. 8. The LHC precision in the LCC1 scenario is extraordinary and unusual; for other scenarios, the LHC is unlikely to determine Ω_χ to better than one or more orders of magnitude. At the same time, even in this “best case scenario,” the LHC determination of Ω_χ leaves open many possibilities. For example, comparison of the LHC result with WMAP/Planck cannot differentiate between a Universe with only neutralino dark matter and a Universe in which dark matter has two components, with neutralinos making up only 80%. Such scenarios are qualitatively distinct, in the sense that the possibility of another component with such significant energy density can lead to highly varying conclusions about the contents of the Universe and the evolution of structure that formed the galaxies we see today.

2.2.2. Mapping the WIMP Universe

WIMPs may appear not only at colliders, but also in dark matter searches. Direct dark matter search experiments look for the recoil of WIMPs scattering off highly shielded detectors. Indirect dark matter searches look for the products, such as positrons, gamma rays or neutrinos, of WIMPs annihilating nearby, such as in the halo, the galactic center, or the core of the Sun.

If WIMPs are discovered at colliders and their thermal relic densities are determined to be cosmologically significant, it is quite likely that they will also be discovered through direct and indirect dark matter search experiments. The requirement of the correct relic density implies that WIMP annihilation was efficient in the early Universe. This suggests efficient annihilation now, corresponding to significant indirect detection rates, and efficient scattering now, corresponding to significant direct detection rates. This rough correspondence is illustrated in Fig. 11.

Direct and indirect dark matter detection rates are subject to uncertainties from both particle physics, through the microphysical properties of dark matter, and astrophysics, through the spatial and velocity distributions of dark matter. If completed, the research program described in Sec. 2.2.1 to pin down the properties of WIMPs will effectively remove particle physics uncertainties. Dark matter search experiments then become probes of dark matter distributions.

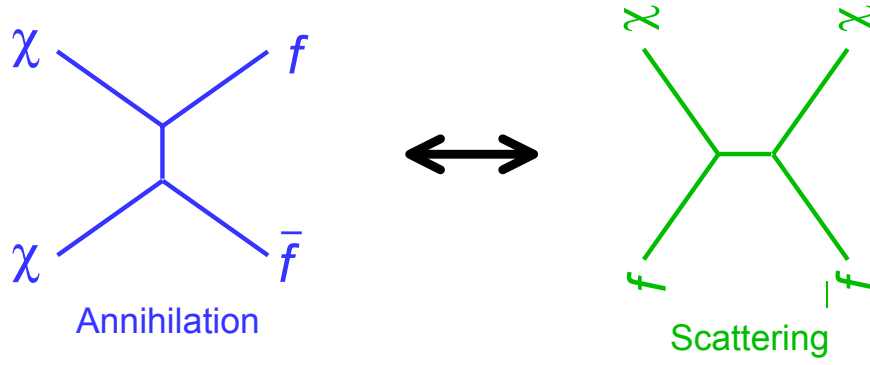


Figure 11: Efficient annihilation, corresponding to large indirect detection rates, is related to efficient scattering, corresponding to large direct detection rates.

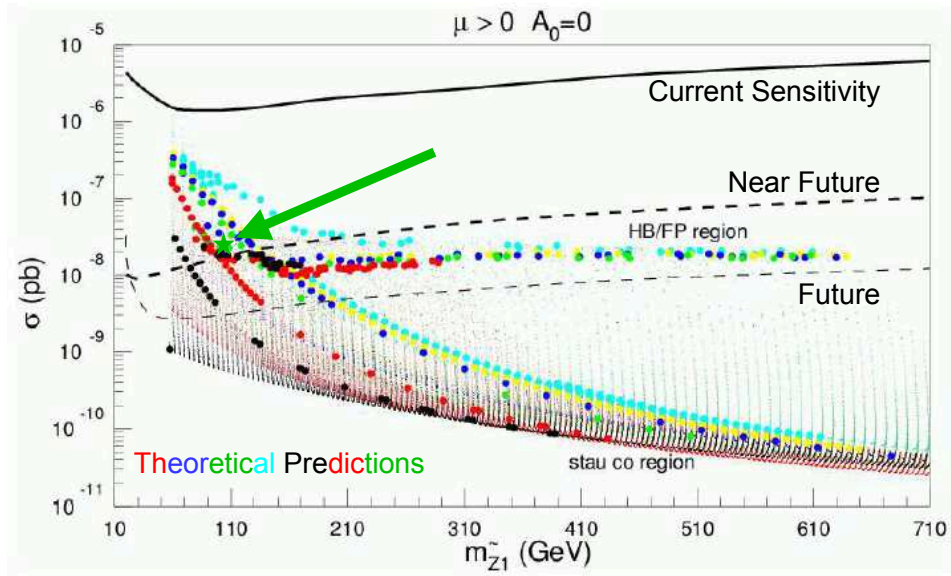


Figure 12: Theoretical predictions for the direct detection neutralino-proton scattering cross section σ , as a function of neutralino mass m_χ , for various mSUGRA models (dots) [39], and the prediction of LCC2 (\star). ILC studies will constrain the values of σ and m_χ to be smaller than the extent of the \star plotting symbol [9].

As an example, consider direct detection. Theoretical predictions of direct detection rates are given in Fig. 12. As is typically done in particle physics studies, a simple dark matter halo profile is assumed throughout this figure. The enormous variation in rates results from particle physics uncertainties alone. LHC and ILC studies will reduce this uncertainty drastically. For example, for LCC2, the dark matter mass will be determined to a GeV at the ILC, and the cross section for neutralino-proton scattering will be determined to $\Delta\sigma/\sigma \lesssim 10\%$ [9]. This constraint is shown in Fig. 12, where the uncertainties are smaller than the extent of the \star plotting symbol.

Once collider constraints effectively remove microphysical uncertainties, the direct detection rates give us information about the local dark matter density and velocity profile. In a similar way, indirect detection rates will provide additional complementary information. For example, experiments such as HESS and GLAST may detect photons dark matter annihilation in the galactic center. Such rates are sensitive to the halo profile at the galactic center, a quantity of great interest at present. The synergy between collider experiments and these dark matter experiments will constrain the phase space distribution of WIMP dark matter in the Universe, with important implications for the formation and evolution of structure.

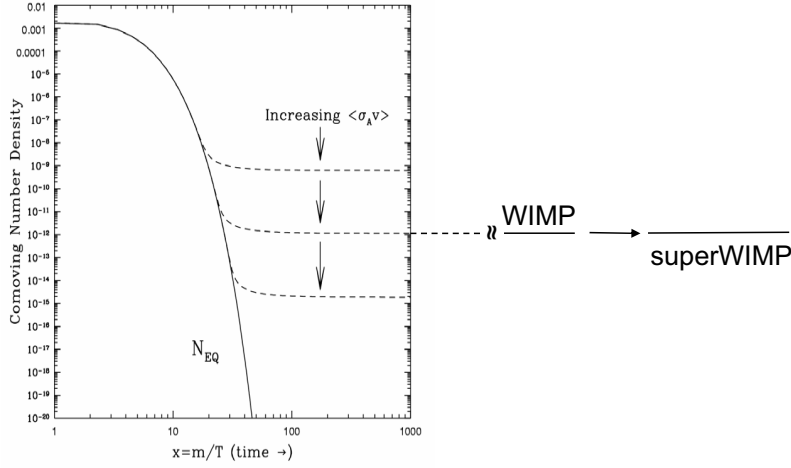


Figure 13: In superWIMP scenarios, a WIMP freezes out as usual, but then decays to a superWIMP, a superweakly-interacting particle that forms dark matter.

2.3. SuperWIMPs

In superWIMP scenarios [40], a WIMP freezes out as usual, but then decays to a stable dark matter particle that interacts *superweakly*, as shown in Fig. 13. The prototypical example of a superWIMP is a weak-scale gravitino produced non-thermally in the late decays of a supersymmetric WIMP, such as a neutralino, charged slepton, or sneutrino [40, 41, 42, 43]. Additional examples include axinos [44] and quintessinos [45] in supersymmetry, Kaluza-Klein graviton and axion states in models with universal extra dimensions [46], and stable particles in models that simultaneously address the problem of baryon asymmetry [47]. SuperWIMPs have all of the virtues of WIMPs. They exist in the same well-motivated frameworks and are stable for the same reasons. In addition, in the natural case that the decaying WIMP and superWIMP have comparable masses, superWIMPs also are naturally produced with relic densities of the desired order of magnitude.

The study of superWIMP dark matter at colliders has common elements with the study of WIMPs, but with key differences. It may also be divided into three (overlapping) stages:

1. SuperWIMP Candidate Identification. Is there evidence for late decays to superWIMPs from collider studies?
2. SuperWIMP Relic Density Determination. What are the superWIMP candidates' predicted relic densities? Can they be significant components or all of dark matter? What are their masses, spins, and other quantum numbers?
3. Mapping the SuperWIMP Universe. Combined with other astrophysical and cosmological results, what can collider studies tell us about astrophysical questions, such as the distribution of dark matter in the Universe?

For Stage 1, collider evidence for superWIMPs may come in one of two forms. Collider experiments may find evidence for charged, long-lived particles. Given the stringent bounds on charged dark matter, such particles presumably decay, and their decay products may be superWIMPs. Alternatively, colliders may find seemingly stable WIMPs, but the WIMP relic density studies described in Sec. 2.2.1 may favor a relic density that is too large, providing evidence that WIMPs decay. These two possibilities are not mutually exclusive. In fact, the discovery of charged long-lived particles with too-large predicted relic density is a distinct possibility and would provide strong motivation for superWIMP dark matter.

In the following subsections, we will explore how well the LHC and ILC may advance Stages 2 and 3.

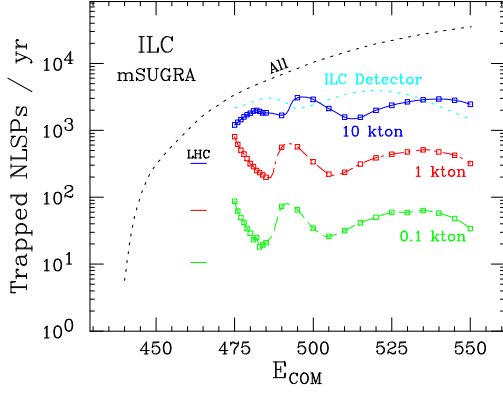
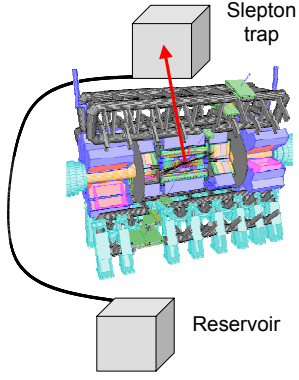


Figure 14: Left: Configuration for slepton trapping in gravitino superWIMP scenarios. Right: The number of sleptons trapped per year at the ILC in 10 kton (solid), 1 kton (dot-dashed), and 0.1 kton (dashed) water traps. The total number of sleptons produced is also shown (upper dotted) along with the number of sleptons trapped in the ILC detector (lower dotted). The trap shape and placement have been optimized and a luminosity of $300 \text{ fb}^{-1}/\text{yr}$ is assumed. The underlying model is minimal supergravity with $M_{1/2} = 600 \text{ GeV}$, $m_0 = 0$, $A_0 = 0$, $\tan\beta = 10$, and $\mu > 0$. The LHC results for this model are as indicated [53].

2.3.1. Relic Density Determination

SuperWIMPs are produced in the late decays of WIMPs. Their number density is therefore identical to the WIMP number density at freeze out, and the superWIMP relic density is

$$\Omega_{\text{superWIMP}} = \frac{m_{\text{superWIMP}}}{m_{\text{WIMP}}} \Omega_{\text{WIMP}}. \quad (10)$$

To determine the superWIMP relic density, we must therefore determine the superWIMP's mass. This is not easy, since the WIMP lifetime may be very large, implying that superWIMPs are typically produced long after the WIMPs have escaped collider detectors.

For concreteness, consider the case of supersymmetry with a stau next-to-lightest supersymmetric particle (NLSP) decaying to a gravitino superWIMP.² The stau is a particle with mass near $M_{\text{weak}} \sim 100 \text{ GeV}$ decaying through gravitational interactions suppressed by the (reduced) Planck mass $M_* \simeq 2.4 \times 10^{18} \text{ GeV}$. On dimensional grounds, we therefore expect its lifetime to be M_*^2/M_{weak}^3 . More precisely, we find

$$\tau(\tilde{\tau} \rightarrow \tau \tilde{G}) = 48\pi M_*^2 \frac{m_{\tilde{G}}^2}{m_{\tilde{\tau}}^5} \left[1 - \frac{m_{\tilde{G}}^2}{m_{\tilde{\tau}}^2} \right]^{-4} \sim 10^4 - 10^8 \text{ s}. \quad (11)$$

This is outlandishly long by particle physics standards. This gravitino superWIMP scenario therefore implies that the signal of supersymmetry at colliders will be meta-stable sleptons with lifetimes of days to months. Such particles will produce highly-ionizing tracks that should be spectacularly obvious at the LHC [48, 49, 50, 51].

At the same time, because some sleptons will be slowly moving and highly-ionizing, they may be trapped and studied [52, 53, 54]. As an example, sleptons may be trapped in water tanks placed outside collider detectors. These water tanks may then be drained periodically to underground reservoirs where slepton decays may be observed in quiet environments. This possibility has been studied in Ref. [53] and is illustrated in Fig. 14.

How many sleptons may be stopped in a reasonably sized trap? The answer is highly model-dependent. The results for one model with 219 GeV sleptons is shown in Fig. 14. At the LHC, hundreds of sleptons may be caught

²If superWIMPs are produced in sufficient numbers to be much of the dark matter, neutralino NLSPs are heavily disfavored, as their late decays invariably violate constraints from BBN and the CMB [40, 42, 43].

each year in a 10 kton trap, assuming a luminosity of $100 \text{ fb}^{-1}/\text{yr}$. These LHC results may be improved significantly if long-lived NLSP sleptons are kinematically accessible at the ILC. For the identical case with 219 GeV sleptons, $\mathcal{O}(1000)$ sleptons may be trapped each year in a 10 kton trap at the ILC, assuming $300 \text{ fb}^{-1}/\text{yr}$. By considering the slightly more general possibility of placing lead or other dense material between the ILC detector and the slepton trap, a further enhancement of an order of magnitude may be possible, allowing up to $\mathcal{O}(10^4)$ sleptons to be trapped per ILC year. These ILC results are made possible by the ability to tune the beam energy to produce slow NLSPs. The ability to prepare initial states with well-known energies and the flexibility to tune this energy are well-known advantages of the ILC. Here, these features are exploited in a qualitatively new way to produce slow sleptons that are easily captured.

If thousands of sleptons are trapped, the slepton lifetime may be determined to the few percent level simply by counting the number of slepton decays as a function of time. The slepton mass will be constrained by analysis of the collider event kinematics. A per cent level measurement of the slepton lifetime given in Eq. (11) therefore implies a high precision measurement of the gravitino mass, and therefore a determination of the gravitino relic density through Eq. (10). As with the case of WIMPs, consistency at the percent level with the observed dark matter relic density will provide strong evidence that dark matter is indeed composed of gravitino superWIMPs.

SuperWIMP quantum numbers and couplings may also be determined through collider studies [55, 56], although, as indicated above, these will typically be determined after or at the same time as the relic density determination, in contrast to the case of WIMPs. For example, an alternative method to determine the gravitino mass is to measure the energy of slepton decay products. This provides a consistency check of the mass determination described above. Alternatively, these two methods, when combined, determine not only $m_{\tilde{G}}$, but also the Planck mass M_* . Given enough events, the gravitino spin may also be constrained to be $3/2$ [55]. The spin and couplings of the gravitino may therefore be determined, showing that the superWIMP is in fact the superpartner of the graviton and that nature is locally supersymmetric.

2.3.2. Mapping the SuperWIMP Universe

Collider studies of superWIMPs will have significant implications for the phase space distribution of dark matter. In fact, the discovery of superWIMPs may resolve current discrepancies and shed light on important and controversial issues in structure formation.

In the standard cosmology, dark matter is assumed to be cold, as is the case with WIMP dark matter. Cold dark matter is remarkably successful in explaining the observed large scale structure down to length scales of $\sim 1 \text{ Mpc}$. Despite its considerable virtues, however, cold dark matter appears to face difficulty in explaining the observed structure on length scales $\lesssim 1 \text{ Mpc}$. Numerical simulations assuming cold dark matter predict, for example, overdense cores in galactic halos [57] and too many dwarf galaxies in the Local Group [58].

These problems may be resolved by superWIMP dark matter [59, 60, 61, 62, 63]. SuperWIMPs are produced with relativistic velocities at late times, as we have seen. They therefore exhibit properties typically associated with warm dark matter, suppressing power on small scales and potentially resolving the problems of cold dark matter mentioned above. The discovery of superWIMP dark matter and the determination of NLSP and superWIMP masses and other relevant parameters at colliders would therefore change fundamentally our understanding of how galaxies were formed and provide a new framework for understanding halo profiles and the distribution of dark matter.

Decays that produce superWIMPs also typically release electromagnetic and hadronic energy. This energy may modify the light element abundances predicted by standard BBN [40, 64, 65, 66, 67] or distort the black body spectrum of the CMB [40, 68, 69, 70]. Collider studies will be able to determine how much energy is released and at what time, providing still more information with important consequences astrophysics.

3. BARYOGENESIS

In addition to sharpening the problems of dark matter, recent cosmological observations have bolstered constraints from BBN to provide tight bounds on the amount of baryons in the Universe. Such progress highlights our ignorance

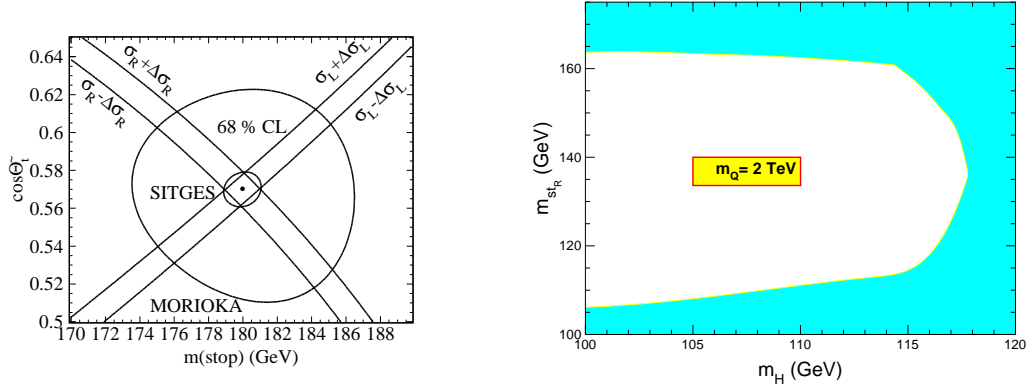


Figure 15: Left: Constraints on top squark masses and mixings from polarized cross section measurements at the ILC [74]. Right: The region of $(m_h, m_{\tilde{t}})$ parameter space (unshaded) in which weak-scale baryogenesis is possible [75].

of the origin of the asymmetry between matter and anti-matter and the mechanism of baryogenesis.

The generation of a net baryon number requires B violation, CP violation, and a period of departure from thermal equilibrium. There are many scenarios for realizing these conditions, with some of the most attractive proposing baryogenesis or leptogenesis at the GUT scale. In such cases, the investigation of baryogenesis and a quantitative explanation for Ω_B will likely be beyond the reach of proposed colliders.

At the same time, all three conditions for baryogenesis may be realized at the weak scale [71]. For example, a baryon excess of the desired size may be generated with weak-scale supersymmetry [72, 73]. This scenario is at present highly constrained, but it provides a concrete example of what is required for the quantitative investigation of baryogenesis at colliders.

In the MSSM, weak-scale baryogenesis requires a Higgs boson mass $m_h \lesssim 118$ GeV and top squark mass below the top quark mass. The region of $(m_h, m_{\tilde{t}})$ parameter space compatible with baryogenesis is shown in Fig. 15. If such a scenario is realized in nature, then, precision Higgs and squark studies will be possible at the ILC. The potential of the ILC for both Higgs and top squark studies has been carefully studied. For example, top squark masses, as well as left-right mixing in the top squark sector may be tightly constrained through polarized cross section measurements. The results of one study are shown in Fig. 15. Top squark mass measurements at the GeV level may favor or disfavor weak-scale baryogenesis.

The full investigation of baryogenesis at colliders requires also the measurement of CP-violating phases. Such studies have been carried out [76, 77, 78, 79, 80]. If light top squarks are produced at the LHC and ILC, such studies may favor or exclude weak-scale baryogenesis. They may even provide quantitative estimates from particle physics of Ω_B , which may be compared with the cosmological observations, leading to implications similar to those for dark matter illustrated in Fig. 10.

4. DARK ENERGY

Recent observations of dark energy provide profound problems for particle physics. In quantum mechanics, an oscillator has zero-point energy $\frac{1}{2}\hbar\omega$. In quantum field theory, the vacuum energy receives contributions of this size from each mode, and so is expected to be $\rho_\Lambda \sim \int^E d^3k \frac{1}{2}\hbar\omega \sim E^4$, where E is the energy scale up to which the theory is valid. Typical expectations for $\rho_\Lambda^{1/4}$ are therefore the weak scale or higher, whereas the observed value is $\rho_\Lambda^{1/4} \sim \text{meV}$. This discrepancy is the cosmological constant problem. Its difficulty stems from the fact that the natural energy scale for solutions is not at high energies yet to be explored, but at low energies that are seemingly well-understood.

Two approaches to the cosmological constant problem are illustrated in Fig. 16. In the first, something, perhaps a symmetry, is assumed to set the cosmological constant to zero. Additional contributions, for example, of size m_ν^4 [81]

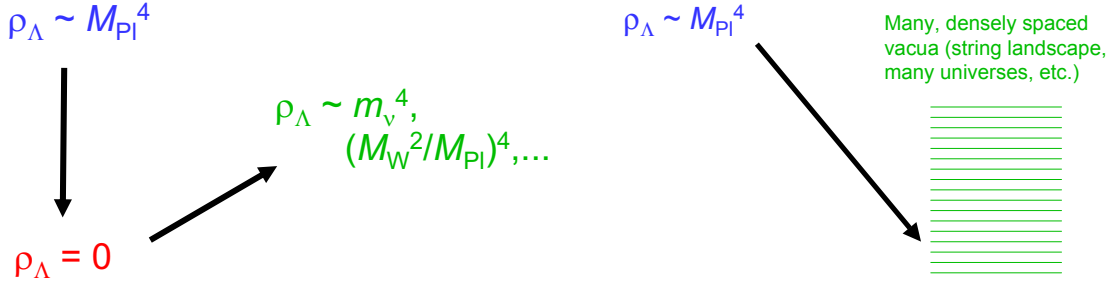


Figure 16: Symmetry (left) and anthropic (right) approaches to the cosmological constant problem.

or $(M_{\text{weak}}^2/M_{\text{Pl}})^4$ [82], bring ρ_Λ up to its observed value. In the second approach, one assumes that there are many possible vacua with energies densely spaced around zero, as possibly provided by string theory [83]. One then hopes that anthropic arguments can explain why values of ρ_Λ near the observed value and not much larger are favored [84].

The symmetry and anthropic approaches to the cosmological constant problem are completely different. Their only similarity is that the more one thinks about either of them, the more one concludes that the other approach must be more promising. There are other proposals, also creative and intriguing, but so far none is particularly compelling.

Perhaps it is not surprising that proposed solutions seem less than satisfactory, however. The cosmological constant is very likely signaling a fundamental problem with our basic ideas, much as the black body problem signaled a problem with classical mechanics at the previous turn-of-the-century. The quantum revolution was decades in the making, and we have had only a few years to puzzle over the modern form of the cosmological constant problem.

Can upcoming colliders provide any insights? It would be pure fancy at this stage to propose an experimental program to solve the cosmological constant problem. On the other hand, the LHC and ILC may contribute in related areas, such as to our understanding of scalar fields and vacuum energy. For example, these colliders may

1. Discover a fundamental scalar particle. Such particles are critical to most discussions of dark energy, from inflation to quintessence to the cosmological constant, but none has yet been observed.
2. Investigate contributions of order $M_{\text{weak}}^4 \sim 10^{60} \rho_\Lambda$ by mapping out the electroweak potential through studies of Yukawa couplings and Higgs self-couplings.
3. Investigate contributions of order $M_{\text{SUSY}}^4 \sim 10^{90} \rho_\Lambda$ by measuring the gravitino mass, perhaps as discussed in Sec. 2.3, and with it, the scale of supersymmetry breaking.
4. Investigate contributions of order $M_{\text{GUT}}^4 \sim 10^{108} \rho_\Lambda$ by extrapolating weak scale measurements to the GUT scale.

It is far from clear that these steps will lead to more compelling explanations of dark energy. At the same time, these steps will constitute progress in closely related topics, and one should not underestimate the power of experimental data to catalyze breakthroughs. We hope that 1 will largely be accomplished when the LHC discovers one or more Higgs bosons, whose properties will then be precisely constrained by the LHC and ILC. For 2, 3, and 4, to the extent the relevant ideas are realized in nature, the ILC will likely be an essential tool.

5. CONCLUSIONS

We live at a doubly exciting time in particle physics. While important questions related to flavor and electroweak symmetry breaking remain, breakthroughs in cosmology have added a whole new layer of fundamental problems requiring particle physics answers. In the next few years, the Tevatron and LHC will begin to explore the weak scale. If there is new physics, experiments at these colliders are likely to discover it, and detailed studies will likely also be possible, especially at the LHC.

What can the ILC add? In particle physics, extensive studies have shown that the ILC can free experimental studies from many theoretical assumptions and simultaneously increase the precision of measurements of many observables. For the cosmological questions explored here, these same characteristics carry over. More than that, however, in many well-motivated examples, the increased precision at the ILC is required to make full use of the precision now obtained in cosmology, and the resulting synergy may lead to *qualitatively* new conclusions, such as the definitive identification of dark matter. The cosmological and astrophysics topics potentially addressed by the ILC are wide-ranging and include dark matter and dark energy, the mechanism of baryogenesis, Big Bang nucleosynthesis, the cosmic microwave background, and the origin of large scale structure. If any of the ideas discussed here is realized in nature, the coming revolution in particle physics will also yield profound insights about the Universe, its contents, and its evolution.

Acknowledgments

It is a pleasure to thank the members of the ALCPG Cosmology Subgroup, particularly my co-editors Marco Battaglia, Norman Graf, Michael Peskin, and Mark Trodden and collaborators Jose Ruiz Cembranos, Konstantin Matchev, Arvind Rajaraman, Bryan Smith, Shufang Su, Fumihiro Takayama, and Frank Wilczek for many contributions to the viewpoints and results summarized here. The work of JLF is supported in part by NSF CAREER grant No. PHY-0239817, NASA Grant No. NNG05GG44G, and the Alfred P. Sloan Foundation.

References

- [1] R. A. Knop *et al.* [The Supernova Cosmology Project Collaboration], *Astrophys. J.* **598**, 102 (2003) [astro-ph/0309368].
- [2] D. N. Spergel *et al.* [WMAP Collaboration], *Astrophys. J. Suppl.* **148**, 175 (2003) [astro-ph/0302209].
- [3] M. Tegmark *et al.* [SDSS Collaboration], *Phys. Rev. D* **69**, 103501 (2004) [astro-ph/0310723].
- [4] T. L. Heath, *A History of Greek Mathematics*, Oxford (1921).
- [5] B. R. Goldstein, *Historia Math.* **11** (4), 411 (1984).
- [6] D. Rawlins, *Isis* **73**, 259 (1982).
- [7] D. Rawlins, *Arch. Hist. Exact Sci.* **26** (3), 211 (1982).
- [8] E. Gulbekian, *Arch. Hist. Exact Sci.* **37** (4), 359 (1987).
- [9] Report of the Cosmology Subgroup, American Linear Collider Physics Group, in preparation.
- [10] R. Gray *et al.*, hep-ex/0507008.
- [11] F. D. Steffen, hep-ph/0507003.
- [12] Y. Mambrini, hep-ph/0507154.
- [13] A. Birkedal *et al.*, hep-ph/0507214.
- [14] S. Kanemura, Y. Okada and E. Senaha, hep-ph/0507259.
- [15] W. de Boer, hep-ph/0508108.
- [16] M. Battaglia and M. E. Peskin, hep-ph/0509135.
- [17] G. Jungman, M. Kamionkowski and K. Griest, *Phys. Rept.* **267**, 195 (1996) [hep-ph/9506380].
- [18] HEPAP LHC/ILC Subpanel, “Discovering the Quantum Universe,” <http://www.linearcollider.org>.
- [19] For a pedagogical review discussing both WIMPs and superWIMPs, see J. L. Feng, eConf **C0307282**, L11 (2003) [hep-ph/0405215]; *Annals Phys.* **315**, 2 (2005).
- [20] H. Goldberg, *Phys. Rev. Lett.* **50**, 1419 (1983);
- [21] G. Servant and T. M. P. Tait, *Nucl. Phys. B* **650**, 391 (2003) [hep-ph/0206071].
- [22] H. C. Cheng, J. L. Feng and K. T. Matchev, *Phys. Rev. Lett.* **89**, 211301 (2002) [hep-ph/0207125].
- [23] J. A. R. Cembranos, A. Dobado and A. L. Maroto, *Phys. Rev. Lett.* **90**, 241301 (2003) [hep-ph/0302041]; *Phys. Rev. D* **68**, 103505 (2003) [hep-ph/0307062].

- [24] H. C. Cheng and I. Low, JHEP **0309**, 051 (2003) [hep-ph/0308199].
- [25] B. C. Allanach, G. Belanger, F. Boudjema and A. Pukhov, JHEP **0412**, 020 (2004) [hep-ph/0410091].
- [26] T. Moroi, Y. Shimizu and A. Yotsuyanagi, hep-ph/0505252.
- [27] F. E. Paige, S. D. Protopescu, H. Baer and X. Tata, hep-ph/0312045.
- [28] P. Gondolo, J. Edsjo, P. Ullio, L. Bergstrom, M. Schelke and E. A. Baltz, JCAP **0407**, 008 (2004) [astro-ph/0406204].
- [29] G. Belanger, F. Boudjema, A. Pukhov and A. Semenov, hep-ph/0405253.
- [30] B. C. Allanach *et al.*, in *Proc. of the APS/DPF/DPB Summer Study on the Future of Particle Physics (Snowmass 2001)* ed. N. Graf, Eur. Phys. J. C **25**, 113 (2002) [eConf **C010630**, P125 (2001)] [hep-ph/0202233].
- [31] G. Weiglein *et al.* [LHC/LC Study Group], hep-ph/0410364.
- [32] J. L. Feng, Int. J. Mod. Phys. A **13**, 2319 (1998) [hep-ph/9803319]; Int. J. Mod. Phys. A **15**, 2355 (2000) [hep-ph/0002055].
- [33] J. L. Feng and M. E. Peskin, Phys. Rev. D **64**, 115002 (2001) [hep-ph/0105100].
- [34] A. Freitas, A. von Manteuffel and P. M. Zerwas, Eur. Phys. J. C **34**, 487 (2004) [hep-ph/0310182].
- [35] J. L. Feng and T. Moroi, Phys. Rev. D **61**, 095004 (2000) [hep-ph/9907319].
- [36] J. L. Feng, K. T. Matchev and T. Moroi, Phys. Rev. Lett. **84**, 2322 (2000) [hep-ph/9908309]; Phys. Rev. D **61**, 075005 (2000) [hep-ph/9909334].
- [37] H. Baer, T. Krupovnickas, S. Profumo and P. Ullio, hep-ph/0507282.
- [38] J. L. Feng, K. T. Matchev and F. Wilczek, Phys. Lett. B **482**, 388 (2000) [hep-ph/0004043]; Phys. Rev. D **63**, 045024 (2001) [astro-ph/0008115].
- [39] H. Baer, C. Balazs, A. Belyaev and J. O’Farrill, JCAP **0309**, 007 (2003) [hep-ph/0305191].
- [40] J. L. Feng, A. Rajaraman and F. Takayama, Phys. Rev. Lett. **91**, 011302 (2003) [hep-ph/0302215]; Phys. Rev. D **68**, 063504 (2003) [hep-ph/0306024].
- [41] J. R. Ellis, K. A. Olive, Y. Santoso and V. C. Spanos, Phys. Lett. B **588**, 7 (2004) [hep-ph/0312262].
- [42] J. L. Feng, S. Su and F. Takayama, Phys. Rev. D **70**, 063514 (2004) [hep-ph/0404198]; Phys. Rev. D **70**, 075019 (2004) [hep-ph/0404231].
- [43] L. Roszkowski and R. Ruiz de Austri, hep-ph/0408227.
- [44] L. Covi, J. E. Kim and L. Roszkowski, Phys. Rev. Lett. **82**, 4180 (1999) [hep-ph/9905212]; L. Covi, H. B. Kim, J. E. Kim and L. Roszkowski, JHEP **0105**, 033 (2001) [hep-ph/0101009].
- [45] X. J. Bi, M. z. Li and X. m. Zhang, Phys. Rev. D **69**, 123521 (2004) [hep-ph/0308218].
- [46] J. L. Feng, A. Rajaraman and F. Takayama, Phys. Rev. D **68**, 085018 (2003) [hep-ph/0307375].
- [47] R. Kitano and I. Low, hep-ph/0503112.
- [48] M. Drees and X. Tata, Phys. Lett. B **252**, 695 (1990).
- [49] J. L. Goity, W. J. Kossler and M. Sher, Phys. Rev. D **48**, 5437 (1993) [hep-ph/9305244].
- [50] A. Nisati, S. Petrarca and G. Salvini, Mod. Phys. Lett. A **12**, 2213 (1997) [hep-ph/9707376].
- [51] J. L. Feng and T. Moroi, Phys. Rev. D **58**, 035001 (1998) [hep-ph/9712499].
- [52] K. Hamaguchi, Y. Kuno, T. Nakaya and M. M. Nojiri, hep-ph/0409248.
- [53] J. L. Feng and B. T. Smith, hep-ph/0409278.
- [54] A. De Roeck, J. R. Ellis, F. Gianotti, F. Moortgat, K. A. Olive and L. Pape, hep-ph/0508198.
- [55] W. Buchmuller, K. Hamaguchi, M. Ratz and T. Yanagida, Phys. Lett. B **588**, 90 (2004) [hep-ph/0402179].
- [56] J. L. Feng, A. Rajaraman and F. Takayama, Int. J. Mod. Phys. D **13**, 2355 (2004) [hep-th/0405248].
- [57] B. Moore, galaxy Nature **370**, 629 (1994); R. A. Flores and J. R. Primack, halos,” Astrophys. J. **427**, L1 (1994) [astro-ph/9402004]; J. J. Binney and N. W. Evans, Mon. Not. Roy. Astron. Soc. **327**, L27 (2001) [astro-ph/0108505]; A. R. Zentner and J. S. Bullock, Phys. Rev. D **66**, 043003 (2002) [astro-ph/0205216]; J. D. Simon *et al.*, Matter-Dominated Astrophys. J. **621**, 757 (2005) [astro-ph/0412035].
- [58] I. A. A. Klypin, A. V. Kravtsov, O. Valenzuela and F. Prada, Astrophys. J. **522**, 82 (1999) [astro-ph/9901240]; A. R. Zentner and J. S. Bullock, Astrophys. J. **598**, 49 (2003) [astro-ph/0304292].
- [59] K. Sigurdson and M. Kamionkowski, Phys. Rev. Lett. **92**, 171302 (2004) [astro-ph/0311486].

- [60] S. Profumo, K. Sigurdson, P. Ullio and M. Kamionkowski, Phys. Rev. D **71**, 023518 (2005) [astro-ph/0410714].
- [61] M. Kaplinghat, astro-ph/0507300.
- [62] J. A. R. Cembranos, J. L. Feng, A. Rajaraman and F. Takayama, hep-ph/0507150.
- [63] K. Jedamzik, M. Lemoine and G. Moulta, astro-ph/0508141.
- [64] R. H. Cyburt, J. R. Ellis, B. D. Fields and K. A. Olive, Phys. Rev. D **67**, 103521 (2003) [astro-ph/0211258].
- [65] K. Jedamzik, Phys. Rev. D **70**, 063524 (2004) [astro-ph/0402344].
- [66] M. Kawasaki, K. Kohri and T. Moroi, Phys. Lett. B **625**, 7 (2005) [astro-ph/0402490]; Phys. Rev. D **71**, 083502 (2005) [astro-ph/0408426].
- [67] J. R. Ellis, K. A. Olive and E. Vangioni, Phys. Lett. B **619**, 30 (2005) [astro-ph/0503023].
- [68] W. Hu and J. Silk, Phys. Rev. Lett. **70**, 2661 (1993).
- [69] D. J. Fixsen, E. S. Cheng, J. M. Gales, J. C. Mather, R. A. Shafer and E. L. Wright, Astrophys. J. **473**, 576 (1996) [astro-ph/9605054].
- [70] R. Lamon and R. Durrer, hep-ph/0506229.
- [71] For a review, see M. Trodden, Rev. Mod. Phys. **71**, 1463 (1999) [hep-ph/9803479].
- [72] M. Carena, M. Quiros, A. Riotto, I. Vilja and C. E. M. Wagner, Nucl. Phys. B **503**, 387 (1997) [hep-ph/9702409].
- [73] M. Carena, M. Quiros, M. Seco and C. E. M. Wagner, Nucl. Phys. B **650**, 24 (2003) [hep-ph/0208043].
- [74] M. Berggren, R. Keranen, H. Nowak and A. Sopczak, hep-ph/9911345.
- [75] M. Quiros, Nucl. Phys. Proc. Suppl. **101**, 401 (2001) [hep-ph/0101230].
- [76] T. Ibrahim and P. Nath, Phys. Rev. D **58**, 111301 (1998) [Erratum-ibid. D **60**, 099902 (1999)] [hep-ph/9807501].
- [77] S. Y. Choi, J. Kalinowski, G. Moortgat-Pick and P. M. Zerwas, Eur. Phys. J. C **22**, 563 (2001) [hep-ph/0108117]; Addendum, Eur. Phys. J. C **23**, 769 (2001) [hep-ph/0202039].
- [78] V. D. Barger, T. Falk, T. Han, J. Jiang, T. Li and T. Plehn, Phys. Rev. D **64**, 056007 (2001) [hep-ph/0101106].
- [79] S. Heinemeyer and M. Velasco, hep-ph/0506267.
- [80] For a brief summary, see J. L. Feng and M. M. Nojiri, hep-ph/0210390.
- [81] See, for example, R. Fardon, A. E. Nelson and N. Weiner, JCAP **0410**, 005 (2004) [astro-ph/0309800].
- [82] See, for example, J. E. Kim and H. P. Nilles, Phys. Lett. B **553**, 1 (2003) [hep-ph/0210402].
- [83] R. Bousso and J. Polchinski, JHEP **0006**, 006 (2000) [hep-th/0004134]; J. L. Feng, J. March-Russell, S. Sethi and F. Wilczek, Nucl. Phys. B **602**, 307 (2001) [hep-th/0005276]; S. Kachru, R. Kallosh, A. Linde and S. P. Trivedi, Phys. Rev. D **68**, 046005 (2003) [hep-th/0301240]; L. Susskind, hep-th/0302219; T. Banks, M. Dine and E. Gorbatov, JHEP **0408**, 058 (2004) [hep-th/0309170]; F. Denef and M. R. Douglas, JHEP **0405**, 072 (2004) [hep-th/0404116]; T. Banks, hep-th/0412129.
- [84] S. Weinberg, Phys. Rev. Lett. **59**, 2607 (1987); M. L. Graesser, S. D. H. Hsu, A. Jenkins and M. B. Wise, Phys. Lett. B **600**, 15 (2004) [hep-th/0407174].